

# Calibration of a LaBr spectrometer for neutron activation measurements in BNCT

Valentina Barletta

<sup>a</sup>Università degli studi di Torino,

## Abstract

The purpose of this study is focused on the characterisation of a LaBr<sub>3</sub>(Ce) detector for gamma-ray spectroscopy. In this application the LaBr<sub>3</sub>(Ce) detector is used to measure the  $\gamma$ -ray emitted by neutron activated materials that compose a spectrometric ensemble for qualification of BNCT neutron fields. The interest in the LaBr<sub>3</sub>(Ce) detector is due to its small size, which allows an easy use and portability, as well as a high count rate measurement capability.

The efficiency and energy calibration of the instrument was carried out using various calibrated point-like sources: <sup>133</sup>Ba, <sup>137</sup>Cs, <sup>60</sup>Co, <sup>152</sup>Eu, <sup>22</sup>Na placed at 20 cm from the detector. Selected element foils (Au, Cu, In, Mn, NaCl, V) were then activated at the LENA reactor in Pavia. The activity of these foils was measured by placing the metal discs in "contact-with" and at 20 cm from the detector. It was thus possible to derive a corrective geometric factor, due to the extended shape of the foils, and to estimate the efficiency of the instrument for this specific (non-point-like) geometry. A software code was then developed to isolate the intrinsic background of the instrument and to perform the energy spectra analysis.

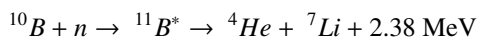
From the acquired measurements, adequate energy resolution was found, but also a limited thermal stability leading to peak shifts over time. However, for time-limited measurements, LaBr<sub>3</sub>(Ce) is an excellent reliable instrument.

## Contents

<b>1 Introduction</b>	<b>1</b>
<b>2 Setup</b>	<b>1</b>
<b>3 Calibration</b>	<b>2</b>
3.1 Energy Calibration . . . . .	2
3.2 Efficiency Calibration at 20 cm . . . . .	2
<b>4 Activation analysis</b>	<b>3</b>
<b>5 Geometric Factor and Efficiency of the detector</b>	<b>3</b>
<b>6 Conclusions</b>	<b>3</b>

## 1. Introduction

Boron Neutron Capture Therapy (BNCT) is an emerging treatment based on the nuclear capture and fission following the irradiation of nonradioactive <sup>10</sup>B with thermal neutrons, which leads to the production of an alpha particle and a recoiling <sup>7</sup>Li:



Treatment begins with an injection of a boron vector, such as BPA (Boronophenylalanine). The vector quickly concentrates in cancer cells and rarely in normal tissues. The cancer is then irradiated with an epithermal neutron beam that will trigger the neutron capture process leading to irreversible damage of the tumor structure. The alpha particle has a short range, therefore preferentially affecting tumor tissues while sparing more distal

normal tissues. It's then important to qualify the neutron beam energy spectrum.

Spectrometric analyses have been conducted on foils activated by a thermal and an epithermal neutron source. A LaBr<sub>3</sub>(Ce) detector, selected mainly for its high mobility, which allows to be easily used in external facilities, has been used. The good energy resolution combined with other features<sup>[1]</sup>, such as high counting efficiency, a high scintillation yield and a short time response, makes this instrument a good detector. However, it's non-negligible the detector's intrinsic noise due to the radioactivity of its constituents, which has to be taken into account in the data analysis.

In this work, we intend to calibrate the detector with a few radioactive sources of known activity placed at 20 cm away from the detector and to obtain the spectrum of a few activated foils.

## 2. Setup

The measurements were performed using a cylindrical LaBr<sub>3</sub>(Ce) scintillation detector of 1.5 in. length and 1.5 in. diameter.

During the calibration phase, the <sup>133</sup>Ba, <sup>137</sup>Cs, <sup>60</sup>Co, <sup>152</sup>Eu and <sup>22</sup>Na  $\gamma$ -ray sources were placed at 20 cm from the detector. Their activities are listed in Table 1. From these measurements, it was possible to derive the energy calibration and also the efficiency at the distance of 20 cm. CHNs are the output channel numbers of the detector.

For activation measurements cylindrical foils of Au, In, Cu, Mn, NaCl, V, with varying diameters (10 mm - 12.7 mm) and thicknesses (30  $\mu$ m - 500  $\mu$ m), were irradiated in the 'Rabbit' channel at the TRiga Mark II nuclear reactor in Pavia<sup>[2]</sup>. The

Table 1: Activity of the sources used for Calibration and their half time life

Source	Activity [kBq]	Half-time [years]
$^{133}\text{Ba}$	$37.00 \pm 0.01$ @ 15/04/2004	10.51
$^{60}\text{Co}$	$18.50 \pm 0.01$ @ 30/01/2018	5.27
$^{137}\text{Cs}$	$19.80 \pm 0.01$ @ 01/07/2017	30.07
$^{152}\text{Eu}$	$6.34 \pm 0.10$ @ 05/07/2022	13.54
$^{22}\text{Na}$	$120.99 \pm 0.01$ @ 08/02/2018	2.60

reactor power was modulated to 300 W (the thermal neutron fluence was approximately  $\phi \approx 1.2 \cdot 10^9 \text{cm}^{-2}$ ). Exposure times were 160 s for NaCl, 100 s for Cu and Mn, 30 s for In and V. These times were evaluated in order to avoid an high detector's dead time.

Due to the high activity of the foils, it was possible to get the measurements at the distance of  $(20.0 \pm 0.1)$  cm from the detector, as well as in contact-with it (approximately  $(2.0 \pm 0.1)$  mm from its surface).

### 3. Calibration

#### 3.1. Energy Calibration

The gamma sources peaks used for the energy calibration have a Gaussian shape, confirmed by a  $\chi^2$  test passed at 5% significance level. Therefore, the channel's peak  $\text{CHN}_{\text{peak}}$  error of each element is the standard deviation  $\sigma_{\text{fit}}$ , achieved from the Gaussian fit. The values obtained are in Table 2.

Table 2: Channel's peak with theoretical Energy for each source

Source	$\text{CHN}_{\text{peak}}$	Energy $E_{\text{th}}$ [keV]
$^{152}\text{Eu}$	$276.0 \pm 5.4$	245
$^{133}\text{Ba}$	$339.0 \pm 5.8$	303
$^{152}\text{Eu}$	$387.0 \pm 6.6$	344
$^{133}\text{Ba}$	$397.0 \pm 6.5$	356
$^{152}\text{Eu}$	$462.0 \pm 6.4$	411
$^{152}\text{Eu}$	$498.0 \pm 7.3$	444
$^{22}\text{Na}$	$572.0 \pm 8.3$	511
$^{137}\text{Cs}$	$736.0 \pm 9.6$	667
$^{152}\text{Eu}$	$(106.2 \pm 1.2) \cdot 10^1$	964
$^{60}\text{Co}$	$(127.9 \pm 1.4) \cdot 10^1$	1170
$^{22}\text{Na}$	$(138.9 \pm 1.5) \cdot 10^1$	1273
$^{60}\text{Co}$	$(143.9 \pm 1.5) \cdot 10^1$	1330

By linking each  $\text{CHN}_{\text{peak}}$  with the respective theoretical energy value  $E_{\text{th}}$ , it's possible to derive the relationship that allows the channels to be operationally converted into energies:

$$\text{CHN} = p_0 \cdot E + p_1 \quad (1)$$

Figure 1 shows the best linear fitting curve of the experimental data with the fitting coefficient values.

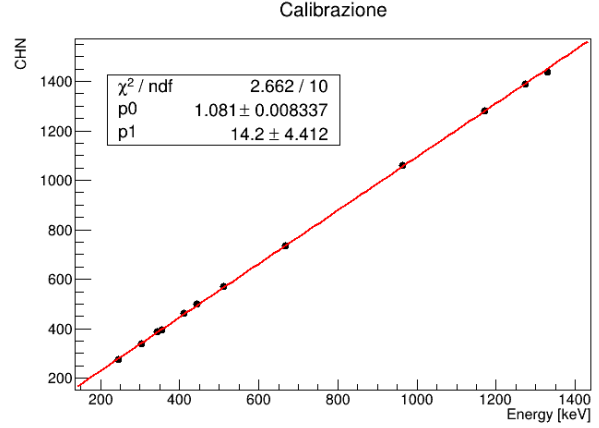


Figure 1: Experimental calibration curve and extraction fit's parameters

#### 3.2. Efficiency Calibration at 20 cm

By the efficiency calibration and the value of counts we can find the foil's activity. However, the detector efficiency cannot be directly evaluated, because the sources used were placed at 20 cm, in order to be considered point-like sources. For this reason, first at all we determined the efficiency at 20 cm,  $\epsilon_{20\text{cm}}$ , of the  $\text{LaBr}_3(\text{Ce})$  detector, and then we estimated the detector efficiency in contact  $\epsilon_{\text{contact}}$  like:

$$\epsilon_{\text{contact}} = \epsilon_{20\text{cm}} \cdot F_{\text{geom}} \quad (2)$$

where  $F_{\text{geom}}$  is the geometric factor (see paragraph 5).

Using the values in Table 1, the source activity  $A$  is estimated as:

$$A = A_0 e^{-\lambda t} \quad (3)$$

where  $A_0$  is the known activity and  $\lambda$  is the decay constant derived from the half-life  $t_{1/2}$ . The  $\epsilon_{20\text{cm}}$  is obtained by the following relationship:

$$\epsilon_{20\text{cm}} = \frac{\text{cps}}{A \cdot \text{BR}} \quad (4)$$

where cps are the counts per second,  $A$  is the activity calculated by (3) and  $\text{BR}$  is the Branching Ratio. We obtained the fit in Figure 2 and its parameters. The functional relationship is:

$$\epsilon_{20\text{cm}} = p_0 \cdot E^{p_1}$$

As expected  $p_1 \approx -1$ , because the efficiency of a gamma ray detector decreases with an increase in gamma ray energy. This is mainly due to two reasons. One of the primary reasons is the decrease in the probability of interaction between the gamma rays and the detector material as the energy of the gamma rays increases. At higher energies, gamma rays tend to pass through the detector without interacting with the material, which reduces the chances of detection. Additionally, at higher energies gamma rays are more likely to interact with the detector material via Compton scattering. This process is less efficient in transferring energy from the gamma ray to the detector, leading to a lower detection efficiency.

We also tried others fitting functions, such as a second order polynomial function, but they seem not to represent the correct experimental trend.

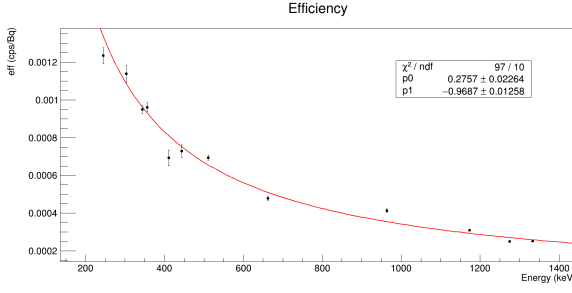


Figure 2: Curve of efficiency at 20 cm and its parameters

#### 4. Activation analysis

After the foils were irradiated at Lena reactor, the radioactivity induced was measured by the detection of the radiation, emitted during the decay of the radionuclide. The following method is used to analyze every foil's peak measured at 20 cm and also in contact with the detector.

The Sensitive Nonlinear Iterative Peak (SNIP)<sup>[3][4]</sup> algorithm has been introduced with the aim to separate different gamma spectrum structure from the photo-peak. See Figure 3.

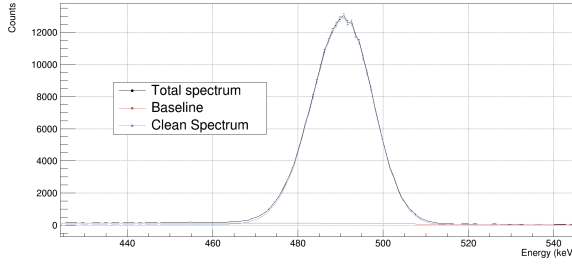


Figure 3: Cu's peak and its baseline in red determined by SNIP

In order to evaluate the foil's activity we needed to identify the correct area under each peak and so we used SNIP to get the Baseline. The Baseline represents the contribution of background from other radioactive sources that are not of interest (it's the "zero" level of the spectrum). From difference between the measurements and the Baseline we could apply the Gaussian fit to each peak. The energy's uncertainty is derived by propagation, while the count's errors are calculated by the root sum square on the error of experimental counts and the baseline's error, both treated as Poissonian uncertainty. All the  $\chi^2$  tests are passed with 5% significance level. The Cu's fit is shown in Figure 4 as an example.

There is an overlap between the V's peak and the La's intrinsic peak of the detector. For this reason we removed that La's peak by subtracting the background noise from the experimental measurements and then we applied SNIP to the result.

#### 5. Geometric Factor and Efficiency of the detector

The Geometric Factor  $F_{geom}$  is the ratio between saturation activity, the maximum activity of a radioactive material, measured at contact and at 20 cm away from the detector. We used

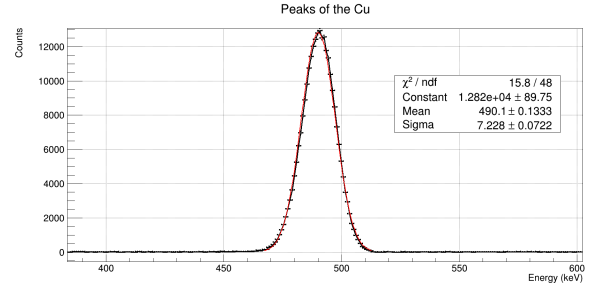


Figure 4: Gaussian fit on Cu's peak and its parameters

the saturation activity to evaluate  $F_{geom}$  in order to obtain it from two comparable measurements. The values and their uncertainty estimated by error's propagation are shown in Table 3. At this point by using (2) and the result of section 3.2 we are able to evaluate the efficiency of the detector and ready to use it in a real BNCT facility.

Table 3: Geometric Factor and its uncertainty

Foil	Geom. Factor	Uncertainty
Au	126.2	5.0
Cu	104.8	3.3
In	87.2	3.2
Mn	97.4	4.3
Na	98.4	1.0
V	106.6	2.3

#### 6. Conclusions

In this work we have calibrated the  $\text{LaBr}_3(\text{Ce})$  detector. The energy calibration was performed placing some sources at 20 cm and obtained the experimental curve that allow to convert channel into energy. The efficiency calibration was determined by multiplying the efficiency estimated at 20 cm and the geometric factor, evaluated from the activation analysis of some foils.

The  $\text{LaBr}_3(\text{Ce})$  is a reliable detector that can be used for neutron spectrometry to characterise a facilities for BNCT.

#### References

- [1] Saint-Gobain, BrilLanCe-380 data sheet.
- [2] L.E.N.A., THE REACTOR TRIGA MARK II, Università di Pavia, <https://lena.unipv.it/en/the-reactor/>.
- [3] V.Arosio, M.Caccia, V.Chmill, A.Ebolese, M.Locatelli, A.Martemianov, M.Pieracci, F.Risigo, R.Santoro, C.Tintori, Background removal procedure based on the SNIP algorithm for  $\gamma$ -ray spectroscopy with the CAEN Educational Kit, (2021).
- [4] Morhac M, Matousek V. Peak clipping algorithms for background estimation in spectroscopic data. Appl Spectrosc. (2008).